HHS Public Access

Author manuscript

Brain Res. Author manuscript; available in PMC 2022 August 27.

Published in final edited form as:

Brain Res. 2020 November 15; 1747: 147062. doi:10.1016/j.brainres.2020.147062.

MRI Detection of Impairment of Glymphatic Function in Rat after Mild Traumatic Brain Injury

Lian Li[1], **Michael Chopp**[1,2], **Guangliang Ding**[1], **Esmaeil Davoodi-Bojd**[1], **Li Zhang**[1], **Qingjiang Li**[1], **Yanlu Zhang**[3], **Ye Xiong**[3], **Quan Jiang**[1]

[1]Department of Neurology, Henry Ford Health System, Detroit, MI 48202, USA.

[2]Department of Physics, Oakland University, Rochester, MI 48309, USA.

[3]Department of Neurosurgery, Henry Ford Health System, Detroit, MI 48208, USA.

Abstract

We investigated the effect of mild traumatic brain injury (mTBI) on the glymphatic pathway using contrast-enhanced magnetic resonance imaging (CE-MRI) and quantified with kinetic parameters obtained from an advanced two-compartment model. mTBI was induced in male Wistar rats using a closed head impact. Animals with and without mTBI (n = 7/group) underwent the identical MRI protocol 10-weeks post-injury, including T2-weighted imaging and 3D T1-weighted imaging with intra-cisterna magna injection of contrast agent (Gd-DTPA). The parameters of infusion rate, clearance rate and clearance time constant, characterizing the kinetic features of glymphatic tracer transport in a living brain, were quantified in multiple brain tissue regions. In the majority of examined regions, our quantification demonstrated significantly reduced infusion and clearance rates, and significantly increased clearance time constant in the mTBI animals compared to the healthy controls. These data indicate that mTBI induces chronic changes in influx and efflux of contrast agent and glymphatic pathway dysfunction. While the reduced efficiency of glymphatic function after mTBI was apparent in brain, regional evaluation revealed heterogeneous glymphatic effects of the mTBI in different anatomical regions. The suppression of glymphatic function, rather than the presence of focal lesions, indicates a persistent injury of the brain after mTBI. Thus, dynamic CE-MRI in conjunction with advanced kinetic analysis may offer a useful methodology for an objective assessment and confirmatory diagnosis of mTBI.

[*]**Corresponding author:** Quan Jiang, PhD, 313-916-8735, 313-916-1324, QJIANG1@hfhs.org. **Mailing address for all authors:** B126, Education & Research Building, Department of Neurology, Henry Ford Hospital, 2799 West Grand Boulevard, Detroit, MI 48202.

Lian Li: Writing - Original Draft, Investigation; Formal analysis; **Michael Chopp:** Writing - Review & Editing; **Guangliang Ding:** Investigation, Methodology; **Esmaeil Davoodi-Bojd:** Software, Formal analysis; **Li Zhang:** Investigation; **Yanlu Zhang:** Investigation; **Ye Xiong:** Investigation; **Qingjiang Li:** Formal analysis; **Quan Jiang:** Supervision, Methodology

Conflicts of interests

The authors have declared that no conflict of interest exists.

Keywords

Glymphatic function; mild traumatic brain injury; contrast agent; kinetic parameter; CE-MRI

1. Introduction

As a brain-wide perivascular network, the glymphatic system allows cerebrospinal fluid (CSF) to exchange with interstitial fluid (ISF), facilitating the clearance of interstitial solutes and wastes from the brain (Benveniste et al., 2019; Jessen et al., 2015; Piantino et al., 2019; Plog and Nedergaard, 2018). Impairment of glymphatic system results in accumulation of pathologic solute within the brain parenchyma, causing metabolite and protein aggregation (Iliff et al., 2012; Iliff et al., 2014; Peng et al., 2016; Plog and Nedergaard, 2018), neuroinflammation and neurodegeneration (Iliff et al., 2014; Plog and Nedergaard, 2018) that are linked to the decline of neurological function (Iliff et al., 2014; Jiang et al., 2017; Ren et al., 2013).

Glymphatic dysfunction has been demonstrated in various neurological diseases (Gaberel et al., 2014; Jessen et al., 2015; Jiang et al., 2017; Peng et al., 2016; Plog and Nedergaard, 2018; Wang et al., 2017), including traumatic brain injury (TBI) (Iliff et al., 2014; Piantino et al., 2019; Ren et al., 2013). Glymphatic function post-TBI has been measured using two-photon imaging (TPI) and histological methods (Iliff et al., 2014; Plog et al., 2015; Plog and Nedergaard, 2018). Although TPI can detect flow at the perivascular level, and histological examination permits cellular and molecular analysis in disparate brain regions, these invasive techniques have their own limitations. For example, TPI with a narrow focal field and shallow focal depth precludes a brain-wide evaluation, histological means does not provide dynamic information (Plog and Nedergaard, 2018). As a non-invasive modality, magnetic resonance imaging (MRI) provides *in vivo,* dynamic and whole-brain as well as spatially localized measurements. Contrast-enhanced MRI (CE-MRI) has been used to visualize and estimate glymphatic activity in the living brain (Benveniste et al., 2017; Gaberel et al., 2014; Iliff et al., 2013; Jiang et al., 2017; Lee et al., 2018; Mestre et al., 2020). However, to our knowledge, there are no CE-MRI investigations on the dynamic variations of glymphatic function, particularly after mild TBI (mTBI), that accounts for at least 75% of brain injuries (Piantino et al., 2019; Shetty et al., 2018).

To date, definitive diagnosis of mTBI with routine neuroimaging modalities remains a challenge due to the absence of a measurable lesion or evidence of injury for most cases (Arciniegas et al., 2005; Borg et al., 2004; Maruta et al., 2010; Shetty et al., 2018). Even though advanced imaging techniques, such as diffusion tensor imaging (DTI) (Sharp and Ham, 2011) and functional MRI (fMRI) (Ptito et al., 2007), permit identification of changes in white matter integrity and task-related activation pattern, respectively, some studies have failed to detect these alterations following mTBI (Lange et al., 2019; Levin et al., 2010; Zhang et al., 2010). By evaluating the metabolic state of the brain, MR spectroscopy (MRS) provides information on the mTBI-induced neuronal/axonal injury as represented by the changes of metabolite concentrations (Cohen et al., 2007; Kirov et al., 2013; Lin et al., 2012). However, neither DTI nor MRS investigations have demonstrated a

consistent trauma-affected cerebral tissue localization in mTBI (Lin et al., 2012), probably attributed to the nature of subtle and diffuse injury. Moreover, traditional neuropsychological tests, that have been widely accepted as standard screening tools for clinical evaluation of abnormalities related to neural impairment, are not sensitive to the effects of mTBI (Ettenhofer and Barry, 2016; Ettenhofer et al., 2020; Maruta et al., 2010). At present, a subjective symptom-based evaluation (Borg et al., 2004; Shetty et al., 2018) has been implemented in the clinical management of mTBI, which may not allow for either accurate identification of mTBI or adequate intervention. The current state of uncertainty for diagnosis of mTBI (Borg et al., 2004; Shetty et al., 2018) creates a compelling need for objective tools to sensitively detect concussion-generated effects that are both technically reliable and clinically applicable. Given that glymphatic suppression following neurodegenerative disorders can be measured using dynamic CE-MRI (Gaberel et al., 2014; Iliff et al., 2013; Jiang et al., 2017; Mestre et al., 2020), a well-established and clinically-relevant imaging technique, the post-mTBI changes in brain function, such as the variance in glymphatic clearance that plays an important role in post-trauma cognitive sequelae (Iliff et al., 2014; Piantino et al., 2019; Ren et al., 2013), may offer a sensitive and confirmatory assessment for this neurological injury.

For mathematical modeling of the glymphatic activity based on CE-MRI, we recently developed an advanced two-compartment kinetic model (Davoodi-Bojd et al., 2019). Instead of the global input function (IF) from the injection site (Lee et al., 2015), we used the local IF obtained from clustering the tissues based on their dynamic responses to the infusion of contrast agent. By fitting the model to the local cerebral regions rather than to the averaged time signal curve (TSC) of the whole brain, more accurate kinetic parameters that characterize the specific features of the dynamic transport of contrast agent in a living brain were then derived. This model has demonstrated an improved capacity to differentiate between diabetic animals and healthy controls (Davoodi-Bojd et al., 2019). Here, using these advanced modeling parameters, we for the first time, perform the present MRI investigation of mTBI. By calculating parametric maps and quantifying kinetic parameters in typical tissue regions across the brain, the present study was designed to reveal whether the impairment of glymphatic pathway function occurs as a result of mTBI and whether the kinetic parameters obtained from our modeling of glymphatic system are sensitive to detect the mTBI-induced brain functional changes.

2. Results

2.1. Structural and glymphatic MRI post-mTBI

Fig. 2 shows one set of T2WIs obtained from a representative rat brain with mTBI. Without MRI evidence of lesion or injury as well as anatomical sign of configuration change on these conventional structural images, the brain appeared normal. However, a time series of T1WIs with Gd-DTPA contrast agent demonstrated the brain alteration in glymphatic function induced by mTBI, as revealed by deviation from normal progression in dynamic transport of contrast agent (Fig. 3). When visually comparing the normal brain (Fig. 3A–3D) with injured brain (Fig. 3E–3H), it was notable that mTBI led to delayed arrival (Fig. 3B vs. 3F), restricted amount and extent (Fig. 3C vs. 3G), and reduced clear-out (Fig. 3D vs.

3H) of contrast agent. This observation was corroborated by the dynamic signal changes for the two groups, measured from symmetric sagittal sections encompassing whole brain (Fig. 3I). Compared to the healthy controls, lower signal intensity within the major experimental period, reflecting reduced amount of contrast agent in the brain, was detected in mTBI group (Fig. 3I), indicative of suppressed glymphatic function.

2.2. mTBI leads to a reduced uptake of contrast agent into the brain

Fig. 4A gives the quantitative results regarding the influence of mTBI on glymphatic influx of contrast agent, as estimated by infusion rate that represents the pace of tracer uptake from CSF into the brain along perivascular spaces. Compared to the healthy animals, significantly reduced values of infusion rate in almost all the measured brain regions (except cerebellum) were found for mTBI animals, suggesting a widespread blockade of glymphatic pathways in the injured brain.

2.3. mTBI leads to a reduced clearance of contrast agent out of the brain

Fig. 4B-4C shows the changes in efficacy of glymphatic efflux on delivered contrast agent post-mTBI, as assessed by clearance rate (Fig. 4B) and clearance time constant (Fig. 4C) that characterize the function of waste drainage from the brain. For examined brain regions, lower clearance rate and higher clearance time constant values were detected in the mTBI group than in the respective control group with differences in the majority of regions reaching statistical significance, indicating a broad decline in glymphatic clearance after mTBI.

2. 4. Regional response to the transport of contrast agent post-mTBI

Parametric quantification from all specific ROIs demonstrated the globally decreased infusion rate, decreased clearance rate and increased clearance time constant in the injured animals compared to the healthy controls (Fig. 4), indicative of an overall suppression of glymphatic influx and efflux function after mTBI, respectively. Although the effects of mTBI on examined brain regions were generally not uniform, the basic patterns for both infusion and clearance rates represented by parametric magnitude in each region largely remained after injury (Fig. 4A-4B). For instance, the highest value was present in hypothalamus, the lowest value in cortex, and the values between them were in the other regions in their order for both groups. However, it is worth noting that a pronounced effect of the mTBI was evident in the olfactory bulb where the parametric values dramatically dropped after injury. As shown in Fig. 4A-4B, infusion rate and clearance rate in olfactory bulb significantly declined from higher values in healthy brain ($p < 0.05$, AVE OB vs. AVE cerebellum) to lower values in injured brain compared to these parametric measures in cerebellum, while such a decline was not found in other regions despite significantly reduced infusion rate and clearance rate present in most regions. In line with these measurements, notable increase in clearance time constant in olfactory bulb (Fig. 4C) from significantly lower value in healthy brain ($p < 0.05$, AVE OB vs. AVE cerebellum) to higher value in injured brain than that in cerebellum was concurrently detected.

3. Discussion

Using CE-MRI and quantified with kinetic parameters obtained from an advanced two-compartment model, we have demonstrated changes of glymphatic pathway function after mTBI. In addition to *in vivo* monitoring with sequential images, the quantification in typical tissue regions across the brain was performed using the parameters that characterize the kinetic features for the dynamic transport of contrast agent in a living brain. Our data show that mTBI affects both influx and efflux of paramagnetic tracer along the perivascular glymphatic pathway. While the reduced efficiency of glymphatic function after a closed head impact is globally apparent, specific anatomical regions seem to be more vulnerable to the impact than the others. The suppression of glymphatic function, rather than the presence of focal lesions, appears to provide a sensitive measure indicating injury to the brain after mTBI.

Due to the lack of imaging and clinical means to effectively identify patients with mTBI, the current diagnosis of mTBI is, therefore, highly dependent upon the information given by the affected individuals' subjective self-report about the characteristics of their acute concussion and the complaints of post-concussion symptoms experienced (Maruta et al., 2010; Shetty et al., 2018). This status of clinical practice has left patients with limited therapeutic options and little or no prognosis, highlighting the need for functional and operational methodologies. Providing objective measures, indicative of abnormalities related to brain injury and subsequent deficits, would help overcome such uncertainty, and thereby, possibly lead to improved diagnosis and management. As demonstrated in the present study, CE-MRI provides a sensitive measurement of the post-mTBI disruption of glymphatic function that has been shown as an important factor in contributing to neurological disabilities (Iliff et al., 2014; Jiang et al., 2017; Ren et al., 2013).

The time series of T1WIs vary concurrently with the dynamic change of tracer concentration in the brain tissue which coincides with continuous CSF transport. Based on the signal variations of T1WIs with time, the tissue uptake and drainage processes of contrast agent that characterize the glymphatic function can then be estimated. As shown in Fig. 3, the sequential images capture both spatial and temporal distribution patterns of delivered tracer in the brain, directly providing visual representations (Fig. 3A–3H) and generating average TSCs for whole brain (Fig. 3I). Even without visible lesions on the structural images (Fig. 2), the suppression of glymphatic function in the brain with mTBI, evidenced by the reduced efficiency and amount of trace transport, can be detected (Fig. 3).

In our advanced glymphatic model, the cluster is created based on tissue response to the infusion of the contrast agent. Using proper criteria (Davoodi-Bojd et al., 2019), a local IF for each cluster obtained from neighboring clusters can then be defined, which largely reduces the errors arising from global IF. This advancement yields more accurate parameters to quantify the kinetics of infused tracer in the brain tissue and improved sensitivity to differentiate between diabetic and non-diabetic animals (Davoodi-Bojd et al., 2019). While infusion rate, herein, represents the performance of glymphatic influx, clearance rate and clearance time constant depict the activity of glymphatic efflux.

For both examined groups, our evaluation with these parameters shows that relatively lower values of infusion rate and clearance rate are present in cortex, hippocampus and thalamus than in hypothalamus, olfactory bulb and cerebellum (Fig. 4A-4B), reflecting the regional heterogeneity in glymphatic transport function (Benveniste et al., 2019; Hadjihambi et al., 2019; Iliff et al., 2013; Jiang et al., 2017). These quantitative results are consistent with the corresponding regional measures in a trauma investigation (Christensen et al., 2020). Importantly, our data demonstrate that mTBI leads to significantly reduced infusion rate and clearance rate (Fig. 4A-4B), corroborated by significantly increased clearance time constant (Fig. 4C), in the majority of examined regions, indicating a global impairment of glymphatic pathway, and hence an overall inefficiency of glymphatic waste clearance. As reported previously, cognitive decline found in various neurological diseases are positively linked to the accumulation of proteins in the brain, including amyloid plaques and tau tangles (Goldstein et al., 2012; Iliff et al., 2014; Jessen et al., 2015; Plog and Nedergaard, 2018). The compromised glymphatic transport function observed after mTBI renders the brain susceptible to the aggregation of waste products, and may accelerate the cognitive dysfunction. Since the glymphatic waste clearance is active primarily during natural sleep (Piantino et al., 2019), it is not surprising that posttraumatic sleep disturbance, one of the most common complaints from patients, may also worsen this posttraumatic glymphatic disruption, thereby contributing to the cognitive decline. Despite the decreased values of both infusion and clearance rates in all measured regions after mTBI (Fig. 4A-4B), the basic pattern represented by the parametric magnitude in each region after injury persists. Compared to the pattern without injury, the pattern after injury exhibits a reduced value version, except in the region of the olfactory bulb where profound declines of both infusion and clearance rates occur because of the injury. In agreement, considerable increase of clearance time constant (Fig. 4C) in the mTBI group was concurrently detected in the same region. The pronounced impact characterized by these parameters on the perivascular glymphatic pathway in olfactory bulb is worth stressing, since some post-injury disorders are closely related to the state of this specific anatomical region (Atighechi et al., 2009; Proskynitopoulos et al., 2016; Swann et al., 2006; Yousem et al., 1996; Yousem et al., 1999).

Olfactory disorder (OD), such as anosmia, is a prevalent complication of head injury (Proskynitopoulos et al., 2016; Swann et al., 2006; Yousem et al., 1996). Although the exact cause of posttraumatic OD remains to be identified, the olfactory bulbs and tracts are found to be the primary sites of involvement, with the damage of these anatomical locations being correlated to the olfactory deficits (Atighechi et al., 2009; Yousem et al., 1999). Regarding the impairment of brain function, our regional measurements show that a closed-skull TBI leads to a more pronounced suppression of glymphatic function in olfactory bulbs, suggesting a higher risk for buildup of neurotoxic substances (Lee et al., 2015; Plog and Nedergaard, 2018) that involve in the subsequent neurodegeneration within the brain parenchyma (Goldstein et al., 2012; Iliff et al., 2014). Thus, our data likely provide new and unique insight into the mechanisms underlying posttraumatic OD, thereby adding to the existing understanding (Atighechi et al., 2009; Proskynitopoulos et al., 2016; Yousem et al., 1999). Again, the present study demonstrates that the disruption of glymphatic function is not necessarily accompanied with MRI visible macroscopic lesion, glymphatic MRI may

therefore offer the pathologic information, not available to conventional MRI, for assessment of patients with posttraumatic OD.

One of major routes for a significant portion of cranial CSF removal from the cranium to peripheral lymphatic system is along the olfactory nerves through the cribriform plate foramina, then, taken up by an extensive network of lymphatic vessels located within the olfactory submucosa and drained into the cervical lymph nodes (Johnston et al., 2004; Kaminski et al., 2012; Nagra et al., 2006). Damage to this olfactory exit route of CSF, such as impairment of olfactory sensory nerves, not only precedes some neurological disorders, but also increases outflow resistance and decreases waste clearance (Johnston et al., 2004; Norwood et al., 2019). Therefore, beyond a local issue, pathologic changes in olfactory bulbs could alter CSF flow dynamics in a widespread brain region (Norwood et al., 2019), thus perturbing solute transport via the glymphatic system. This concept seems to be substantiated by our present observation that with the most severe degree found in olfactory bulbs, a global glymphatic suppression is present in the mTBI-injured brain.

There are several limitations in this study. First, we only examined male rats, rather than both sexes, despite the ostensible gender differences in response to TBI (Dick, 2009; Dillard et al., 2017; Helmer et al., 2014). This is because, in this proof of principle study, we relied on our extensive cognitive (Zhang et al., 2018) and histological (Zhang et al., 2019) data acquired from the same mTBI model in male animals. Secondly, we only performed our cross-sectional study at the chronic stage post-mTBI with persistent cognitive sequelae (Zhang et al., 2018). While multiple measurements at earlier time points following the injury need separate groups of animals, longitudinal evaluations reveal the dynamic alterations of glymphatic function. In addition, the animals with sham surgery without impact were not included in our study since there is no histological (e.g., tissue damage) and functional (e.g., mNSS) evidence of brain injury in the mTBI model (Zhang et al., 2018; Zhang et al., 2019). As a preliminary glymphatic MRI study on mTBI, however, our purpose is to demonstrate that glymphatic MRI combined with kinetic evaluation provide a useful tool for sensitive detection of brain functional change after mTBI. We, therefore, primarily selected the same animal model and gender with which to conduct our investigation at an injury stage when cognitive dysfunction is present, at least partially attributed to the impairment of glymphatic function (Goldstein et al., 2012; Iliff et al., 2014; Jessen et al., 2015; Plog and Nedergaard, 2018). Further studies focusing on the changes of glymphatic function as a function of time post-mTBI, and for different sexes and ages are clearly needed.

In summary, CE-MRI is sensitive to the chronic changes of glymphatic function after mTBI in male young rats. Rather than at the acute time, the persistent post-concussive sequelae, including sleep, physical, cognitive and emotional symptoms, usually occur at the chronic stage when the diagnosis and corresponding intervention are most needed. Glymphatic MRI is therefore a powerful tool, applicable to the clinic for detecting the brain functional change related to chronic mTBI. With kinetic parameters that characterize the dynamic features of perivascular glymphatic transport, the post-injury suppression in glymphatic influx and efflux of contrast agent can be separately and accurately quantified. Despite an overall compromised efficiency of glymphatic function occurring after injury, our quantitative evaluation reveals the heterogeneous effects of a closed head impact on different anatomical

regions. Dynamic CE-MRI in conjunction with advanced kinetic analysis may provide a useful methodology for an objective assessment and confirmatory diagnosis of mTBI.

4. Experimental procedures

All experimental procedures were conducted in accordance with the NIH Guide for the Care and Use of Laboratory Animals and approved by the Institutional Animal Care and Use Committee of Henry Ford Health System.

4.1. Animals and mTBI mode

Male Wistar rats (~ 400g) were used in the current study. Prior to the injury procedure, rats were randomized to two groups: injury or control group (n = 7/group). Only the animals in the injury group were subjected to brain impact. mTBI was induced using a widely-employed model of closed head cortical impact, as previously described (Zhang et al., 2018; Zhang et al., 2019). In brief, the rats were initially anesthetized with 4% isoflurane and maintained with 1.0% - 1.5% isoflurane in 70% N_2O and 30% O_2 via a nose mask throughout the surgical period. Rectal temperature was maintained at 37°C ± 0.5°C using a feedback-regulated water heating system. On the shaved and disinfected skin over the cranial vault, a midline incision (2 cm) was made to expose the skull. A stainless-steel disk (diameter = 10 mm, thickness = 3 mm) was mounted on the parietal bone (midline between bregma and lambda) with cyanoacrylic glue to prevent skull fracture. The animal was supported by a foam bed and placed in a prone position directly under the hollow Plexiglass tube. Closed head injury was induced by dropping a cylindrical column of segmented brass (450 g) through the tube from a height of 1 m onto the disk fixed to the skull vault. After impact, the metal disk was removed and the incision was closed with sterile 4–0 sutures. This model produces injury in the brain (Zhang et al., 2019) and results in chronic neurological deficits (Zhang et al., 2018).

4.2. MR imaging and data processing

MR imaging was performed with a 7T system (Bruker-Biospin, Billerica, MA, US) (Ding et al., 2018). A birdcage type coil was used as the transmitter and a quardrature half-volume coil as the receiver. The animal was securely fixed on a MR-compatible holder equipped with an adjustable nose cone for administration of anesthetic gases and stereotaxic ear bars to immobilize the head. For reproducible positioning of the animal in the magnet, a fast gradient echo imaging sequence was used at the beginning of each MRI session. During image acquisition, anesthesia was maintained by a gas mixture of N_2O (70%) and O_2 (30%) with 1.0% - 1.5% isoflurane (Piramal Inc., Bethiehem, PA, US), and rectal temperature was kept at 37 ± 0.5ºC using a feedback controlled air heating blower (Rapid Electric, Brewster, NY, US).

Rats with and without mTBI underwent the identical whole-brain MRI protocol at the same time point of 10-weeks post-injury. T2-weighted imaging (T2WI) (TE = 8, 16, 24, 32, 40, 48, 56, 64, 72 and 80 ms, TR = 4 s, FOV = 32×32 mm^2, matrix = 128×128, 13 slices, thickness = 1 mm) was measured for detection of brain tissue changes. To monitor the dynamic influx and clean-out process, 3D T1-weighted imaging (T1WI) (TE = 4 ms, TR =

18 ms, flip angle = 12°, FOV = 32×32×16 mm^3, matrix = 256×192×96) with contrast agent of Gd-DTPA was acquired. The time series of T1WI scanning continued for 6 hours, starting with three baseline scans followed by intra-cisterna magna Gd-DTPA (21mM concentration) delivery via the indwelling catheter at a constant infusion rate of 1.6 μl/min over 50 min (Iliff et al., 2013; Jiang et al., 2017).

The detailed procedures regarding MRI data processing and map calculation have been previously described (Davoodi-Bojd et al., 2019). Briefly, the sequential images for each animal were co-registered to its first volume to correct the motion that occurred during the scan. For comparison, images for the studied animals should be in the common spatial space. To this end, 3D T1WIs for all animals were co-registered to a standard reference template. Following these pre-processes, brain voxels were clustered into similar regions based on their dynamic responses to the infusion of contrast agent, while the derivative of time signal curves (TSCs), instead of the actual TSCs, were used to ensure that the cluster was created depending on the dynamics of tracer movement only. With the average TSC for each cluster that represents the retention of infused tracer as a function of time in the tissue region, parameters featuring the kinetics of tracer uptake and clearance within the cluster were calculated. Herein, infusion rate is defined by the rate of signal increase from the point immediately after three baseline scans to the peak in the accumulation phase of the TSC, while clearance rate is defined by the rate of signal decrease from the peak to the end of experiment in the relaxing phase of the TSC. The clearance time constant was obtained by fitting a one exponential model to the relaxing phase of the TSC (Davoodi-Bojd et al., 2019). After calculating these kinetic parameters in every single cluster from its average TSC, parametric maps of infusion rate, clearance rate and clearance time constant for whole brain were then generated.

4.3 Quantification and statistical analysis

To quantify the glymphatic transport of contrast agent in the brain, regions of interest (ROIs) encompassing typical brain tissue areas (including cortex, hippocampus, thalamus, hypothalamus, olfactory bulb and cerebellum) were created on the fixed coronal and sagittal sections of 3D T1WI (Fig. 1). With these ROIs, measurements were conducted on the parametric maps and averaged in each ROI for different groups. Results are presented as mean ± standard error. To detect the effect of mTBI on the glymphatic function in these specific brain regions characterized by the kinetic parameters, a two-sample t-test was performed with $p < 0.05$ inferred for statistical significance.

Acknowledgments

This work was supported by NIH grants RF1 AG057494 (Jiang & Li Zhang), RO1 NS108463 (Jiang).

References

Arciniegas DB, Anderson CA, Topkoff J, McAllister TW, 2005. Mild traumatic brain injury: a neuropsychiatric approach to diagnosis, evaluation, and treatment. Neuropsychiatr Dis Treat. 1, 311–27. [PubMed: 18568112]

Atighechi S, Salari H, Baradarantar MH, Jafari R, Karimi G, Mirjali M, 2009. A comparative study of brain perfusion single-photon emission computed tomography and magnetic resonance imaging in patients with post-traumatic anosmia. Am J Rhinol Allergy. 23, 409–12. [PubMed: 19671257]

Benveniste H, Lee H, Ding F, Sun Q, Al-Bizri E, Makaryus R, Probst S, Nedergaard M, Stein EA, Lu H, 2017. Anesthesia with Dexmedetomidine and Low-dose Isoflurane Increases Solute Transport via the Glymphatic Pathway in Rat Brain When Compared with High-dose Isoflurane. Anesthesiology. 127, 976–988. [PubMed: 28938276]

Benveniste H, Liu X, Koundal S, Sanggaard S, Lee H, Wardlaw J, 2019. The Glymphatic System and Waste Clearance with Brain Aging: A Review. Gerontology. 65, 106–119. [PubMed: 29996134]

Borg J, Holm L, Cassidy JD, Peloso PM, Carroll LJ, von Holst H, Ericson K, 2004. Diagnostic procedures in mild traumatic brain injury: results of the WHO Collaborating Centre Task Force on Mild Traumatic Brain Injury. J Rehabil Med. 61–75. [PubMed: 15083871]

Christensen J, Wright DK, Yamakawa GR, Shultz SR, Mychasiuk R, 2020. Repetitive Mild Traumatic Brain Injury Alters Glymphatic Clearance Rates in Limbic Structures of Adolescent Female Rats. Sci Rep. 10, 6254. [PubMed: 32277097]

Cohen BA, Inglese M, Rusinek H, Babb JS, Grossman RI, Gonen O, 2007. Proton MR spectroscopy and MRI-volumetry in mild traumatic brain injury. AJNR Am J Neuroradiol. 28, 907–13. [PubMed: 17494667]

Davoodi-Bojd E, Ding G, Zhang L, Li Q, Li L, Chopp M, Zhang Z, Jiang Q, 2019. Modeling glymphatic system of the brain using MRI. Neuroimage. 188, 616–627. [PubMed: 30578928]

Dick RW, 2009. Is there a gender difference in concussion incidence and outcomes? Br J Sports Med. 43 Suppl 1, i46–50. [PubMed: 19433425]

Dillard C, Ditchman N, Nersessova K, Foster N, Wehman P, West M, Riedlinger B, Monasterio E, Shaw B, Neblett J, 2017. Post-concussion symptoms in mild traumatic brain injury: findings from a paediatric outpatient clinic. Disabil Rehabil. 39, 544–550. [PubMed: 26971917]

Ding G, Chopp M, Li L, Zhang L, Davoodi-Bojd E, Li Q, Zhang Z, Jiang Q, 2018. MRI investigation of glymphatic responses to Gd-DTPA infusion rates. J Neurosci Res. 96, 1876–1886. [PubMed: 30272825]

Ettenhofer ML, Barry DM, 2016. Saccadic Impairment Associated With Remote History of Mild Traumatic Brain Injury. J Neuropsychiatry Clin Neurosci. 28, 223–31. [PubMed: 27019067]

Ettenhofer ML, Gimbel SI, Cordero E, 2020. Clinical validation of an optimized multimodal neurocognitive assessment of chronic mild TBI. Ann Clin Transl Neurol. 7, 507–516. [PubMed: 32207241]

Gaberel T, Gakuba C, Goulay R, Martinez De Lizarrondo S, Hanouz JL, Emery E, Touze E, Vivien D, Gauberti M, 2014. Impaired glymphatic perfusion after strokes revealed by contrast-enhanced MRI: a new target for fibrinolysis? Stroke. 45, 3092–6. [PubMed: 25190438]

Goldstein LE, Fisher AM, Tagge CA, Zhang XL, Velisek L, Sullivan JA, Upreti C, Kracht JM, Ericsson M, Wojnarowicz MW, Goletiani CJ, Maglakelidze GM, Casey N, Moncaster JA, Minaeva O, Moir RD, Nowinski CJ, Stern RA, Cantu RC, Geiling J, Blusztajn JK, Wolozin BL, Ikezu T, Stein TD, Budson AE, Kowall NW, Chargin D, Sharon A, Saman S, Hall GF, Moss WC, Cleveland RO, Tanzi RE, Stanton PK, McKee AC, 2012. Chronic traumatic encephalopathy in blast-exposed military veterans and a blast neurotrauma mouse model. Sci Transl Med. 4, 134ra60.

Hadjihambi A, Harrison IF, Costas-Rodríguez M, Vanhaecke F, Arias N, Gallego-Durán R, Mastitskaya S, Hosford PS, Olde Damink SWM, Davies N, Habtesion A, Lythgoe MF, Gourine AV, Jalan R, 2019. Impaired brain glymphatic flow in experimental hepatic encephalopathy. J Hepatol. 70, 40–49. [PubMed: 30201461]

Helmer KG, Pasternak O, Fredman E, Preciado RI, Koerte IK, Sasaki T, Mayinger M, Johnson AM, Holmes JD, Forwell LA, Skopelja EN, Shenton ME, Echlin PS, 2014. Hockey Concussion Education Project, Part 1. Susceptibility-weighted imaging study in male and female ice hockey players over a single season. J Neurosurg. 120, 864– 72. [PubMed: 24490839]

Iliff JJ, Wang M, Liao Y, Plogg BA, Peng W, Gundersen GA, Benveniste H, Vates GE, Deane R, Goldman SA, Nagelhus EA, Nedergaard M, 2012. A paravascular pathway facilitates CSF flow through the brain parenchyma and the clearance of interstitial solutes, including amyloid beta. Sci Transl Med. 4, 147ra111.

Iliff JJ, Lee H, Yu M, Feng T, Logan J, Nedergaard M, Benveniste H, 2013. Brain-wide pathway for waste clearance captured by contrast-enhanced MRI. J Clin Invest. 123, 1299–309. [PubMed: 23434588]

Iliff JJ, Chen MJ, Plog BA, Zeppenfeld DM, Soltero M, Yang L, Singh I, Deane R, Nedergaard M, 2014. Impairment of glymphatic pathway function promotes tau pathology after traumatic brain injury. J Neurosci. 34, 16180–93. [PubMed: 25471560]

Jessen NA, Munk AS, Lundgaard I, Nedergaard M, 2015. The Glymphatic System: A Beginner's Guide. Neurochem Res. 40, 2583–99. [PubMed: 25947369]

Jiang Q, Zhang L, Ding G, Davoodi-Bojd E, Li Q, Li L, Sadry N, Nedergaard M, Chopp M, Zhang Z, 2017. Impairment of the glymphatic system after diabetes. J Cereb Blood Flow Metab. 37, 1326–1337. [PubMed: 27306755]

Johnston M, Zakharov A, Papaiconomou C, Salmasi G, Armstrong D, 2004. Evidence of connections between cerebrospinal fluid and nasal lymphatic vessels in humans, non-human primates and other mammalian species. Cerebrospinal Fluid Res. 1, 2. [PubMed: 15679948]

Kaminski M, Bechmann I, Pohland M, Kiwit J, Nitsch R, Glumm J, 2012. Migration of monocytes after intracerebral injection at entorhinal cortex lesion site. J Leukoc Biol. 92, 31–9. [PubMed: 22291210]

Kirov II, Tal A, Babb JS, Reaume J, Bushnik T, Ashman TA, Flanagan S, Grossman RI, Gonen O, 2013. Proton MR spectroscopy correlates diffuse axonal abnormalities with post-concussive symptoms in mild traumatic brain injury. J Neurotrauma. 30, 1200–4. [PubMed: 23339670]

Lange RT, Yeh PH, Brickell TA, Lippa SM, French LM, 2019. Postconcussion symptom reporting is not associated with diffusion tensor imaging findings in the subacute to chronic phase of recovery in military service members following mild traumatic brain injury. J Clin Exp Neuropsychol. 41, 497–511. [PubMed: 30871410]

Lee H, Xie L, Yu M, Kang H, Feng T, Deane R, Logan J, Nedergaard M, Benveniste H, 2015. The Effect of Body Posture on Brain Glymphatic Transport. J Neurosci. 35, 11034–44. [PubMed: 26245965]

Lee H, Mortensen K, Sanggaard S, Koch P, Brunner H, Quistorff B, Nedergaard M, Benveniste H, 2018. Quantitative Gd-DOTA uptake from cerebrospinal fluid into rat brain using 3D VFA-SPGR at 9.4T. Magn Reson Med. 79, 1568–1578. [PubMed: 28627037]

Levin HS, Wilde E, Troyanskaya M, Petersen NJ, Scheibel R, Newsome M, Radaideh M, W T, Yallampalli R, Chu Z, Li X, 2010. Diffusion tensor imaging of mild to moderate blast-related traumatic brain injury and its sequelae. J Neurotrauma. 27, 683–94. [PubMed: 20088647]

Lin AP, Liao HJ, Merugumala SK, Prabhu SP, Meehan WP 3rd, Ross BD, 2012. Metabolic imaging of mild traumatic brain injury. Brain Imaging Behav. 6, 208–23. [PubMed: 22684770]

Maruta J, Lee SW, Jacobs EF, Ghajar J, 2010. A unified science of concussion. Ann N Y Acad Sci. 1208, 58–66. [PubMed: 20955326]

Mestre H, Du T, Sweeney AM, Liu G, Samson AJ, Peng W, Mortensen KN, Staeger FF, Bork PAR, Bashford L, Toro ER, Tithof J, Kelley DH, Thomas JH, Hjorth PG, Martens EA, Mehta RI, Solis O, Blinder P, Kleinfeld D, Hirase H, Mori Y, Nedergaard M, 2020. Cerebrospinal fluid influx drives acute ischemic tissue swelling. Science. 367.

Nagra G, Koh L, Zakharov A, Armstrong D, Johnston M, 2006. Quantification of cerebrospinal fluid transport across the cribriform plate into lymphatics in rats. Am J Physiol Regul Integr Comp Physiol. 291, R1383–9. [PubMed: 16793937]

Norwood JN, Zhang Q, Card D, Craine A, Ryan TM, Drew PJ, 2019. Anatomical basis and physiological role of cerebrospinal fluid transport through the murine cribriform plate. Elife. 8.

Peng W, Achariyar TM, Li B, Liao Y, Mestre H, Hitomi E, Regan S, Kasper T, Peng S, Ding F, Benveniste H, Nedergaard M, Deane R, 2016. Suppression of glymphatic fluid transport in a mouse model of Alzheimer's disease. Neurobiol Dis. 93, 215–25. [PubMed: 27234656]

Piantino J, Lim MM, Newgard CD, Iliff J, 2019. Linking Traumatic Brain Injury, Sleep Disruption and Post-Traumatic Headache: a Potential Role for Glymphatic Pathway Dysfunction. Curr Pain Headache Rep. 23, 62. [PubMed: 31359173]

Plog BA, Dashnaw ML, Hitomi E, Peng W, Liao Y, Lou N, Deane R, Nedergaard M, 2015. Biomarkers of traumatic injury are transported from brain to blood via the glymphatic system. J Neurosci. 35, 518–26. [PubMed: 25589747]

Plog BA, Nedergaard M, 2018. The Glymphatic System in Central Nervous System Health and Disease: Past, Present, and Future. Annu Rev Pathol. 13, 379–394. [PubMed: 29195051]

Proskynitopoulos PJ, Stippler M, Kasper EM, 2016. Post-traumatic anosmia in patients with mild traumatic brain injury (mTBI): A systematic and illustrated review. Surg Neurol Int. 7, S263–75. [PubMed: 27213113]

Ptito A, Chen JK, Johnston KM, 2007. Contributions of functional magnetic resonance imaging (fMRI) to sport concussion evaluation. NeuroRehabilitation. 22, 217–27. [PubMed: 17917172]

Ren Z, Iliff JJ, Yang L, Yang J, Chen X, Chen MJ, Giese RN, Wang B, Shi X, Nedergaard M, 2013. 'Hit & Run' model of closed-skull traumatic brain injury (TBI) reveals complex patterns of post-traumatic AQP4 dysregulation. J Cereb Blood Flow Metab. 33, 834–45. [PubMed: 23443171]

Sharp DJ, Ham TE, 2011. Investigating white matter injury after mild traumatic brain injury. Curr Opin Neurol. 24, 558–63. [PubMed: 21986682]

Shetty T, Nguyen JT, Cogsil T, Tsiouris AJ, Niogi SN, Kim EU, Dalal A, Halvorsen K, Cummings K, Zhang T, Masdeu JC, Mukherjee P, Marinelli L, 2018. Clinical Findings in a Multicenter MRI Study of Mild TBI. Front Neurol. 9, 836. [PubMed: 30405511]

Swann IJ, Bauza-Rodriguez B, Currans R, Riley J, Shukla V, 2006. The significance of post-traumatic amnesia as a risk factor in the development of olfactory dysfunction following head injury. Emerg Med J. 23, 618–21. [PubMed: 16858094]

Wang M, Ding F, Deng S, Guo X, Wang W, Iliff JJ, Nedergaard M, 2017. Focal Solute Trapping and Global Glymphatic Pathway Impairment in a Murine Model of Multiple Microinfarcts. J Neurosci. 37, 2870–2877. [PubMed: 28188218]

Yousem DM, Geckle RJ, Bilker WB, McKeown DA, Doty RL, 1996. Posttraumatic olfactory dysfunction: MR and clinical evaluation. AJNR Am J Neuroradiol. 17, 1171–9. [PubMed: 8791933]

Yousem DM, Geckle RJ, Bilker WB, Kroger H, Doty RL, 1999. Posttraumatic smell loss: relationship of psychophysical tests and volumes of the olfactory bulbs and tracts and the temporal lobes. Acad Radiol. 6, 264–72. [PubMed: 10228615]

Zhang K, Johnson B, Pennell D, Ray W, Sebastianelli W, Slobounov S, 2010. Are functional deficits in concussed individuals consistent with white matter structural alterations: combined FMRI & DTI study. Exp Brain Res. 204, 57–70. [PubMed: 20496060]

Zhang Y, Chopp M, Gang Zhang Z, Zhang Y, Zhang L, Lu M, Zhang T, Winter S, Brandstätter H, Mahmood A, Xiong Y, 2018. Prospective, randomized, blinded, and placebo-controlled study of Cerebrolysin dose-response effects on long-term functional outcomes in a rat model of mild traumatic brain injury. J Neurosurg. 129, 1295–1304. [PubMed: 29303438]

Zhang Y, Chopp M, Zhang ZG, Zhang Y, Zhang L, Lu M, Zhang T, Winter S, Doppler E, Brandstäetter H, Mahmood A, Xiong Y, 2019. Cerebrolysin Reduces Astrogliosis and Axonal Injury and Enhances Neurogenesis in Rats After Closed Head Injury. Neurorehabil Neural Repair. 33, 15–26. [PubMed: 30499355]

Highlights

- Dynamic CE-MRI is sensitive to the chronic changes of glymphatic function after mTBI.
- mTBI affects both influx and efflux of contrast agent along the glymphatic pathway.
- mTBI induces an overall suppression of glymphatic function at the chronic stage.
- mTBI results in the heterogeneous glymphatic effects on different anatomical regions.
- Glymphatic MRI in conjunction with advanced kinetic analysis provide a useful methodology for an objective assessment and confirmatory diagnosis of mTBI.

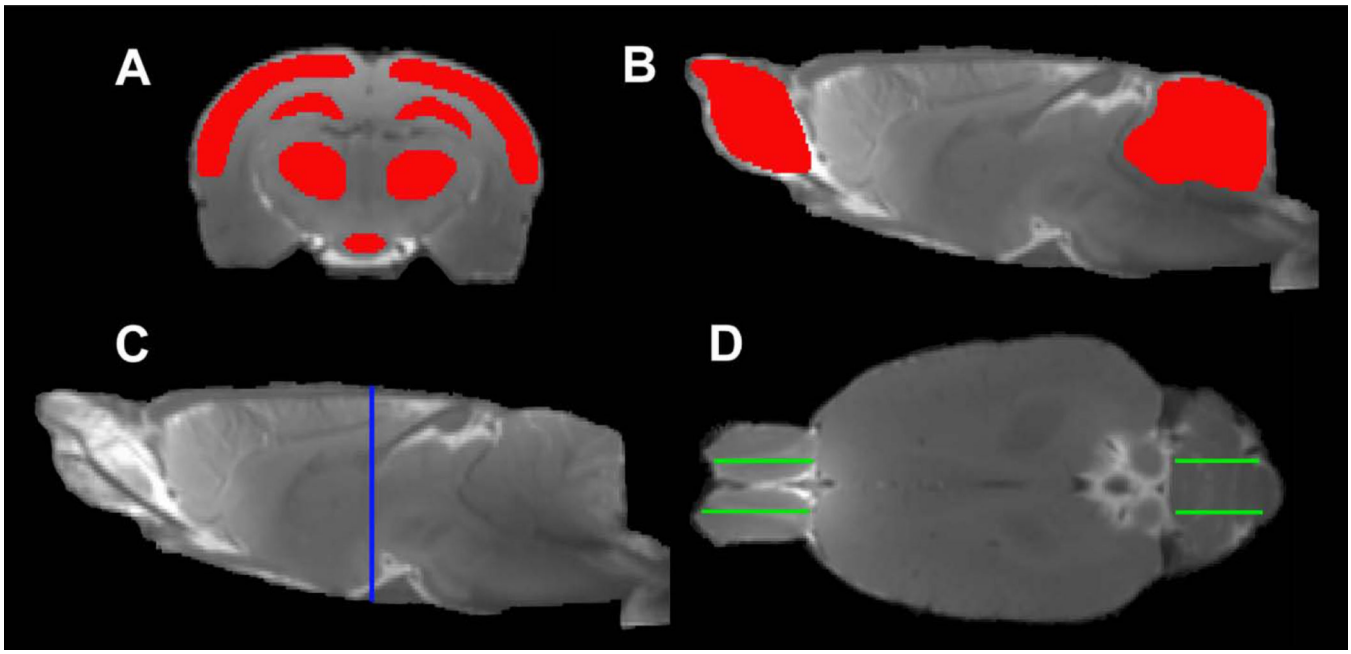

Fig. 1.

Regions of interest (ROIs) (red in **A**, **B**) on the coronal (**A**) and sagittal (**B**) sections, and the corresponding locations seeing on the sagittal (**C**, blue line) and axial (**D**, green lines) sections, respectively. The symmetric ROIs in the same tissue structure (**D**, green lines in OB and cerebellum) provide average measurements.

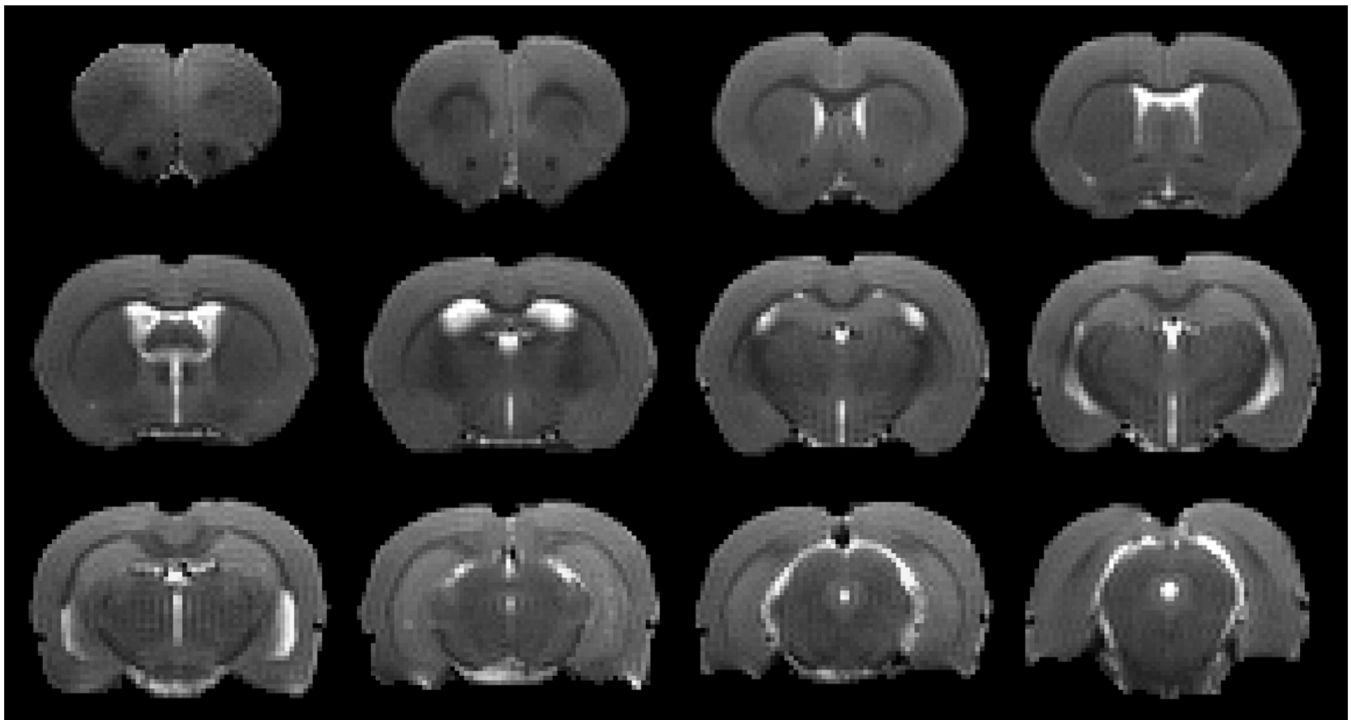

Fig. 2.

A set of T2WIs obtained from a representative rat brain after a closed head impact (10-weeks post-mTBI). No abnormality is present.

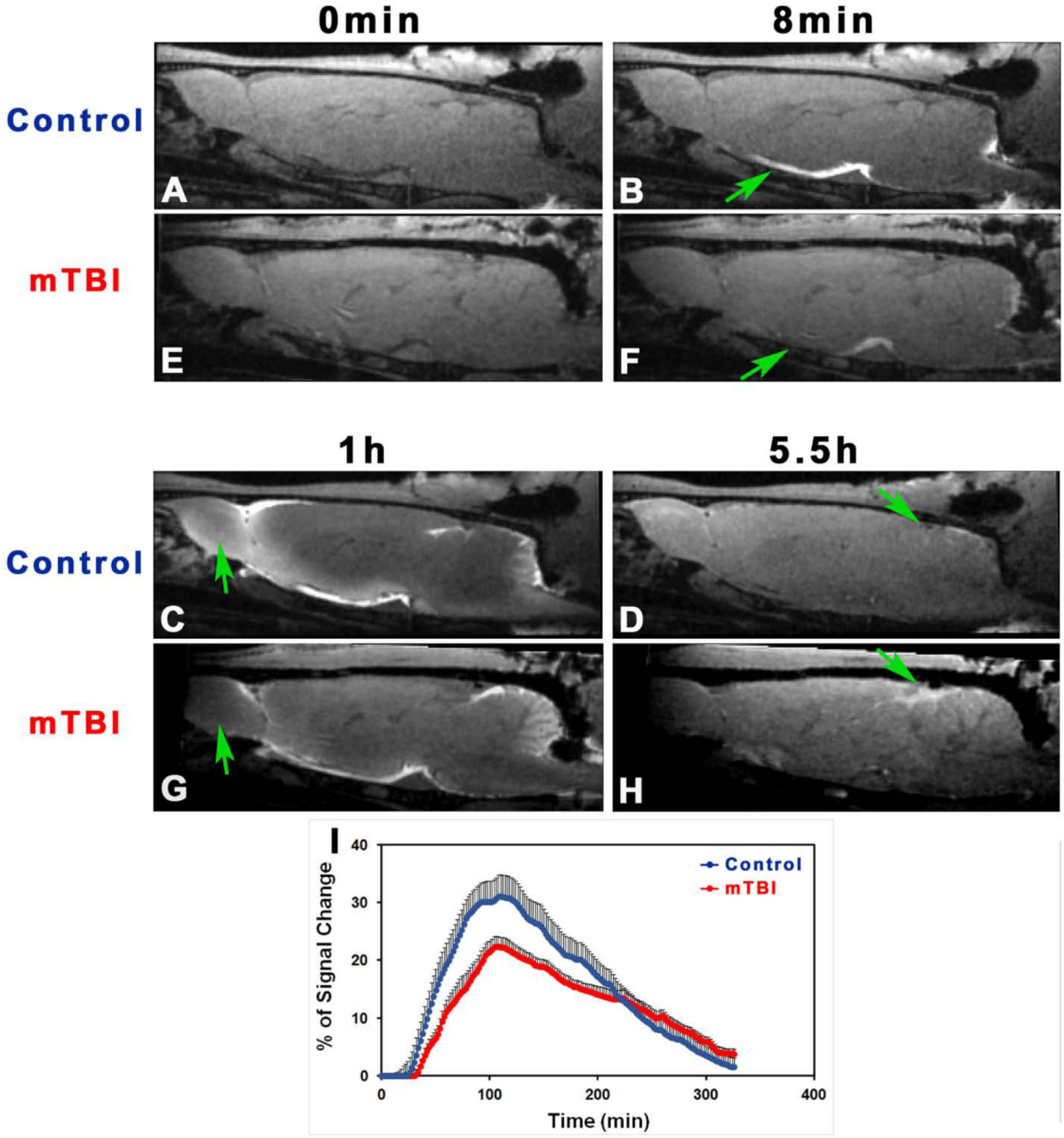

Fig. 3.

T1WIs (**A**-**H**) at typical time points showing the progressive transport of contrast agent in the brain with (**E**-**H**) and without (**A**-**D**) injury (10-weeks post-mTBI). As indicated by arrows, mTBI leads to delayed arrival (**B** vs. **F**), restricted amount and extent (**C** vs. **G**), and reduced clean-out (**D** vs. **H**) of contrast agent compared to the healthy control. Group average TSCs (**I**, n = 7/group) obtained from symmetric sagittal sections encompassing whole brain present the signal changes along time. Within the major experimental period,

lower signal intensity, reflecting reduced amount of contrast agent in the brain, is detected in the mTBI group than in the control group.

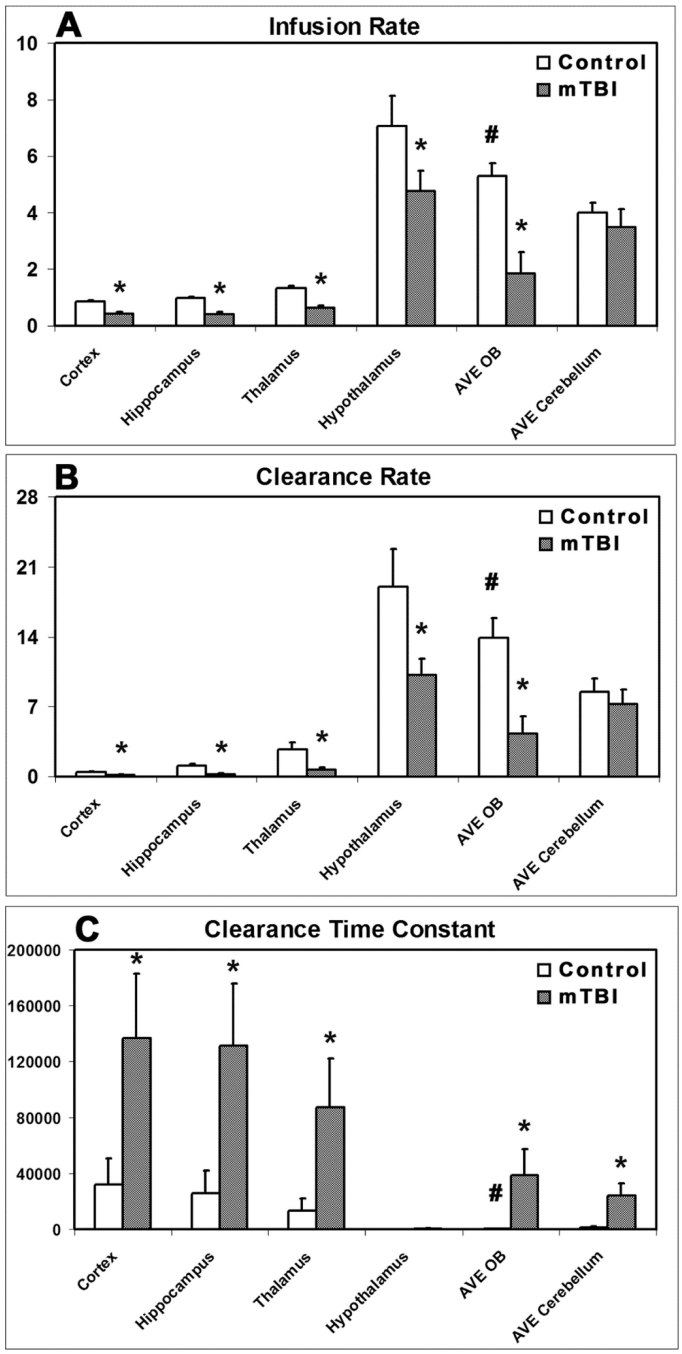

Fig. 4.

Group comparison of infusion rate (**A**), clearance rate (**B**) and clearance time constant (**C**) in examined regions (n = 7/group, 10-weeks post-mTBI). *****: $p < 0.05$, control vs. mTBI in the same region; #: $p < 0.05$, AVE OB vs. AVE cerebellum in the control group.